Effect of Torrefaction on Bio-oil Upgrading over HZSM-5. Part 2: Byproduct Formation and Catalyst Properties and Function

ARTICLE *in* ENERGY & FUELS · NOVEMBER 2012

Impact Factor: 2.79 · DOI: 10.1021/ef301695c

5 AUTHORS, INCLUDING:

Roger Norris Hilten
University of Georgia
22 PUBLICATIONS **263** CITATIONS
SEE PROFILE

James Robert Kastner
University of Georgia
63 PUBLICATIONS **828** CITATIONS
SEE PROFILE

Sudhagar - Mani
University of Georgia
64 PUBLICATIONS **1,578** CITATIONS
SEE PROFILE

K.C. Das
University of Georgia
131 PUBLICATIONS **3,433** CITATIONS
SEE PROFILE

energy&fuels

Article

pubs.acs.org/EF

Effect of Torrefaction on Bio-oil Upgrading over HZSM-5. Part 2: Byproduct Formation and Catalyst Properties and Function

Roger N. Hilten,* Richard A. Speir, James R. Kastner, Sudhagar Mani, and K. C. Das

College of Engineering, Driftmier Engineering Center, University of Georgia, Athens, Georgia 30202, United States

ABSTRACT: A three-step bio-oil production process involving torrefaction pretreatment (225, 250, or 275 °C at 20 min hold time), pyrolysis (500 °C, two heating rates), and secondary catalytic processing over HZSM-5 (at 400, 450, or 500 °C) was studied to determine how treatments affected byproduct formation and catalyst properties and function. Torrefaction pretreatment significantly reduced average yields (%, w/w of feed) of reactor char (100% reduction), catalyst coke (21.4%), and catalyst tar (8.1%) relative to the best-case conditions using non-torrefied feedstock. The yields of chemical components, including levoglucosan, formic acid, acetic acid, and 5-hydroxymethylfurfural (5-HMF), were significantly reduced in intermediate fast-pyrolysis bio-oil (FPO) derived from torrefied feedstock, while for intermediate slow-pyrolysis bio-oil (SPO), yields of levoglucosan, acetic acid, and 5-HMF were reduced. However, in terms of concentration, only furfural showed a significant correlation with the torrefaction temperature. Both furfural and formic acid indicated correlations with coke formation, although these were negative correlations. For formic acid, a decreased coke yield with an increasing concentration was attributed to the formation of H_2 from the thermal decomposition. Combined coke, char, and tar yield significantly decreased with an increasing torrefaction temperature, decreasing formic acid, acetic acid, and furfural concentrations, and an increasing levoglucosan concentration to a minimum of 14.4% (w/w of bio-oil feed). Torrefaction also increased catalyst effectiveness for minimizing changes to pore size, pore volume, and surface area upon upgrading FPO but reduced effectiveness for SPO processing. Torrefaction of biomass prior to slow pyrolysis more effectively maintained weak and strong acid site density after catalytic processing, although no clear effect of torrefaction was seen for FPO-processing catalysts.

INTRODUCTION

Catalytic cracking has been shown to improve the quality of pyrolysis oils generated from a variety of high oxygen content biomass.[1−6] Developed by the petroleum industry to crack and rearrange high-boiling-point, high-molecular-weight petroleum crude oil fractions to predominantly gasoline and other light hydrocarbons,[7] cracking can be applied similarly to improve the characteristics of biomass-derived pyrolysis liquids.

Acidic zeolites with ion-exchange capacity and size selectivity functionality, such as HZSM-5, have been shown to effectively deoxygenate bio-oil feedstocks and form desirable end-products, including small alkanes and aromatics,[4,7,8] as well as a number of undesirable byproducts, such as catalyst coke. Coke formation on zeolitic catalysts can be extensive, as much as 29% (w/w of feed),[4,5] and many studies have sought methods to reduce coke formation.[3,7,9] Vitolo et al.[10] indicated much more modest levels of coke (4.2−6.7%, w/w of feed) using HZSM-5 to process Swedish pine at 500 °C. According to Rao et al.,[11] the amount of coke generated during modern crude oil processing is around 5% (w/w of crude oil feed). If coke formation from bio-oil processing can remain in the range for crude oil processing, the transition to processing biomass-derived feedstock in existing petroleum units will not be problematic.

One way to minimize coke formation on zeolite catalysts is to remove coke precursors from the oil prior to upgrading. Compounds that are thought to promote coke formation include aldehydes, oxyphenols, furfural, and lignin-derived oligomers.[6,12] Other studies involving hydrotreating of bio-oil[13−16] have indicated that the carbohydrate fraction, of which the major component is levoglucosan, is also a major contributor to coke formation. There is currently very little research that attempts to remove coke precursors from bio-oil prior to upgrading. Pretreatment of biomass by torrefaction, a low-temperature (200−320 °C), anoxic heating process, prior to pyrolysis is one potential way to remove coke precursors from bio-oil prior to upgrading and, thus, reduce coke formation and improve bio-oil quality.

Hemicellulose decomposition has been proposed to occur in the temperature range from 200 to 300 °C, with drying occurring prior to 200 °C. For cellulose, the range of decomposition is 300−400 °C, and for lignin, the range of decomposition is 250−500 °C.[17] Thus, in the normal temperature range for torrefaction (200−320 °C), biomass is effectively dried and hemicellulose is devolatilized and decomposed along with some cellulose and lignin.[18] Meng et al.[19] observed that torrefaction pretreatment resulted in a fast pyrolysis bio-oil with a larger fraction of pyrolytic lignin (oxyphenols and phenolic oligomers), implying that torrefaction effectively removed hemicellulose and some cellulose components.

During torrefaction, a variety of reactive and acidic intermediate components, including organic acids (e.g., acetic, formic, and propionic) and aldehydes (e.g., formaldehyde, hydroxyacetaldehyde, acetaldehyde, and furfural), is evolved.[20−23] The removal of acetic acid, which is derived from the deacetylation of the xylan component of hemi-

Received: October 17, 2012
Revised: November 19, 2012
Published: November 19, 2012

Table 1. Feedstock Characteristics for Torrefied and Untorrefied PC Biomass

	feedstock characteristics (%, w/w dry basis)				
parameter	PC (average ± 95% CI)	PC T100 (average ± 95% CI)	PC T225 (average ± 95% CI)	PC T250 (average ± 95% CI)	PC T275 (average ± 95% CI)
yield[a]	100 ± N/A	86.0 ± N/A	71.2 ± N/A	69.7 ± N/A	55.6 ± N/A
moisture[b]	14.0 ± 0.32	0.03 ± 0.02	0.48 ± 0.28	0.35 ± 0.10	0.01 ± 0.02
volatiles	82.0 ± 0.42	81.4 ± 0.02	80.0 ± 0.22	77.9 ± 1.20	72.3 ± 0.47
ash	0.2 ± 0.03	0.30 ± 0.04	0.36 ± 0.03	0.39 ± 0.05	0.20 ± 0.16
fixed carbon	17.9 ± 0.39	18.3 ± 0.02	19.6 ± 0.24	21.7 ± 1.15	27.5 ± 0.31
C	46.9 ± 0.2	46.9 ± 0.2	48.3 ± 0.5	48.4 ± 0.1	53.3 ± 0.6
H	5.98 ± 0.1	5.98 ± 0.1	5.88 ± 0.1	5.83 ± 0.1	5.6 ± 0
N	0.45 ± 0.1	0.45 ± 0.1	0.88 ± 0.2	0.82 ± 0.1	1 ± 0.3
S	0 ± 0	0 ± 0	0 ± 0	0 ± 0	0 ± 0
O[c]	46.3 ± 0.2	46.3 ± 0.2	44.6 ± 0.2	44.6 ± 0.1	39.9 ± 0.5
HHV[d] (MJ kg^{-1})	18.6 ± 0.1	18.6 ± 0.1	19.1 ± 0.1	19.1 ± 0.1	21.1 ± 0.3

[a]Yields are calculated versus air-dried PC biomass. [b]Wet basis. [c]By difference. [d]Calculated following Channiwala and Parikh.

cellulose,[17,19] is particularly advantageous because it occurs in a relatively high concentration (~10%), catalyzes a number of aging reactions, and decomposes to form coke during catalytic upgrading processing.[21,24,25] In addition, a number of aldehydes are evolved in measurable concentrations during torrefaction, including formaldehyde, acetaldehyde, syringaldehyde, hydroxyacetaldehyde, and furfurals.[21] Joo et al.[26] showed that formaldehyde, in particular, effectively deactivated strong acid sites on HZSM-5 catalysts. Although some reactive gases produced during the torrefaction phase of pyrolysis have been shown to generate coke on acid catalysts, leading to deactivation,[12,27] and despite the fact that the 2008 NSF/DOE Roadmap[28] has indicated that the impact of torrefaction on thermochemical processing should be investigated, to date, no research has been performed to determine the effect of torrefaction as a pretreatment for pyrolysis, followed by catalytic cracking of produced bio-oil. Torrefaction, when coupled with pyrolysis and catalytic cracking, could provide synergistic effects not realized with drying and/or catalytic treatment alone.

In addition, after upgrading bio-oil from non-torrefied feedstock, residual organic acids end up in the product, causing high acidity (low pH) and corrosivity. Thus, it is proposed that pyrolyzing a hemicellulose-depleted feedstock will result in bio-oils containing less acetic acid and other reactive compounds, resulting in reduced coke formation during HZSM-5-catalyzed cracking. The main objective of this study was to investigate the effects of torrefaction pretreatment on the concentration of proposed coke precursors, on the formation of byproducts, including coke, reactor char, and tar, and on catalyst properties and function as a result of byproduct formation upon processing fast- and slow-pyrolysis bio-oils generated from torrefied pine wood.

EXPERIMENTAL SECTION

A multi-step process was used to generate bio-oil from loblolly pine. Steps included feedstock pretreatment (via torrefaction), pyrolysis (fast and slow heating rates), and secondary catalytic cracking. Torrefaction was performed in a pilot-scale (500 kg per batch) rotating kiln torrefaction unit. Torrefied feedstock was pyrolyzed under fast-pyrolysis conditions (<5 s reaction time) in a continuous flow fluidized-bed pyrolysis unit (FBPU). Slow pyrolysis was performed in a batch slow-pyrolysis unit (BSPU). For catalytic cracking, a fixed-bed plug flow reactor (PFR) unit was used to process bio-oil generated via the fast pyrolysis of pine chip (PC) or torrefied pine chip (TPC) biomass.

Loblolly pine biomass was supplied by Plum Creek Timber Company (Athens, GA) in the form of delimbed and debarked logs harvested in northeastern Georgia. Logs were then cut into sections prior to being chipped in a Vermeer 1230 brush chipper (Vermeer Corporation, Pella, IA). Material was then sorted in a Royer model 42 power screener (Royer Industries, Oshkosh, WI) using a 0.64 cm screen to collect reject material. Particles larger than 5 cm were hand-removed. Chipped biomass was left to air-dry in a covered, open shed for 6 months prior to further processing.

Biomass Pretreatment. Biomass pretreatment via torrefaction was performed at 225, 250, and 275 °C (named T225, T250, and T275), a commonly used temperature range for the partial or complete removal of hemicellulose, in a pilot-scale rotary kiln. During the torrefaction process, approximately 100 kg of air-dried PCs (2−5 cm particle size and 14 ± 0.32% moisture content) was loaded into the rotary kiln. The kiln was a 3 m^3 octagonal-shaped mild steel reactor externally heated by a 22.9 MW (1.3 MMBTU h^{-1}) natural gas burner. The volume of the PCs comprised less than 1 m^3 of the reactor volume. Details of the torrefaction unit are provided elsewhere.[29]

Once each end temperature was reached, a holding time of 20 min was maintained to drive complete devolatilization of components. After torrefaction, the resulting torrefied feedstocks (PC T225, PC T250, and PC T275) were characterized along with air- and oven-dried PC (PC T100) biomass (see Table 1), ground to 1−2 mm, and then subjected to fast pyrolysis at 500 °C or left in chip form for slow-pyrolysis processing, as described in the following section.

Bio-oil Production. Bio-oil was generated by pyrolyzing oven-dried (100 °C for 4 h, a.k.a. T100) or torrefied (225, 250, or 275 °C, a.k.a. T225, T250, and T275) PC biomass at 500 °C in the FBPU (>100 °C s^{-1} heating rate) or the BSPU (0.13 °C s^{-1} heating rate). Prior to fast pyrolysis, the biomass particle size was reduced in a hammer mill to 1−2 mm. Details of the FBPU reactor are provided elsewhere.[29]

The batch slow pyrolysis reactor used was a cubical (20 × 20 × 20 cm) stainless-steel (grade 316L) reactor. Two 1.3 cm ports allowed for the introduction of inert gas and the removal of evolved gases and vapors. For slow pyrolysis runs, approximately 3 kg of dry PCs was placed in the reactor and the reactor was placed in a single set point electric furnace (Thermolyne model 30400, BarnStead International, Dubuque, IA). A low heating rate (8 °C min^{-1}) was applied until the reactor reached a final internal temperature of 500 °C, and evolved vapors were condensed in an ice bath vapor trap. The two-phase liquid obtained was separated in a gravity separation funnel. The heavier, non-aqueous lower phase was considered the product. Sub-samples of condensed bio-oil from fast and slow pyrolysis (heavier organic phase) were taken for analysis, while the remaining sample was used in the subsequent catalytic cracking process described below.

Bio-oil Catalytic Cracking. Previously produced and phase-separated (slow pyrolysis only) bio-oil was injected continuously into the PFR maintained at 400, 450, or 500 °C in a tube furnace. The PFR

dx.doi.org/10.1021/ef301695c | Energy Fuels 2013, 27, 844−856

consisted of a 2.4 cm inner diameter reactor with a 38 cm length. A 15 cm preheater section was incorporated into the reactor to ensure that bio-oil was in vapor phase prior to crossing a 10 g catalyst bed (28.5 cm^3) that was held in place by stainless-steel screens and quartz wool above and below the bed. Bio-oil was pumped using a peristaltic pump that maintained a feed rate of 1.5 $cm^3\ min^{-1}$ (~100 g h^{-1} at an average bio-oil feedstock density of 1.1 g cm^{-3}), corresponding to a weight hourly space velocity (WHSV, h^{-1}) of 10 h^{-1}. WHSV was calculated as the mass flow rate (g h^{-1}) of liquid feed divided by the catalyst mass (g). These reaction conditions corresponded to a liquid hourly space velocity [LHSV = reactant liquid flow rate ($cm^3\ h^{-1}$)/reactor volume (cm^3)] of 3.2 h^{-1}. The catalyst/oil ratio (C/O, weight of the catalyst divided by the weight of oil fed) ranged from 0.34 to 0.65. The catalyst contact time [3600/(WHSV × C/O)] thus ranged from 554 to 1058 s. Given a carrier gas flow rate of 50 $cm^3\ min^{-1}$, gas-phase residence time in the catalytic zone (V = 28.5 cm^3) was approximately 34 s.

Catalyst Preparation. The catalyst, HZSM-5, was produced by calcining NH_4-ZSM-5 (Zeolyst International, CBV 5524 G) at 550 °C for 4 h in air to produce the hydrogen form, HZSM-5, resulting in stronger acid pore sites. The pH was measured by mixing catalyst in water at a 50:50 ratio and then measuring the pH of the water using a standard pH probe. As a result of the calcining process, the pH was reduced from 4.98 to 3.06. The NH_4-ZSM-5 catalyst was received from the manufacturer as a fine powder. To minimize the pressure drop across the catalyst bed, the catalyst was granulated by thoroughly mixing with water in a beaker, drying at 100 °C, physical crumbling, and sieving to the desired size, ~2−4 mm.

After calcination, granulation, and drying, catalyst surface characteristics (surface area, average pore radius, and pore volume) were determined using a surface area analyzer (Quantachrome Autosorb, model 1-C, Boynton Beach, FL) by measuring N_2 adsorption/desorption isotherms. The adsorption and desorption isotherms were obtained at −196 °C (77 K), with the Brunauer−Emmett−Teller (BET) surface area calculated from the linear portion of the multipoint BET plot. The micropore volume and external surface area were evaluated using the *t*-plot method, and the pore size distribution was obtained using the Brunauer−Joyner−Halenda (BJH) model. Characteristics of as-received and prepared catalysts are provided in Table 2.

Table 2. Characteristics of As-Received and Prepared HZSM-5 Catalysts

property	as-received	prepared
cation form	NH_4^+	H^+
Si/Al	50	50
particle size (mm)	0.005	2−4
surface area ($m^2\ g^{-1}$)	425	345
average pore radius (Å)	N/A	10.8
pore volume ($cm^3\ g^{-1}$)	N/A	0.19

Experimental design parameters are provided in Table 3. Including control samples that were dried at 100 °C and subsequently subjected to the catalytic process, 32 bio-oil types were produced and labeled by pretreatment (drying or torrefaction) temperature (T100, T225, T250, or T275), pyrolysis heating rate [fast-pyrolysis oil (FPO) or slow-pyrolysis oil (SPO)], and catalytic upgrading temperature (U400, U450, or U500). Each process condition was run in triplicate for a total of 96 samples. Intermediate bio-oils produced from pyrolysis, FPO and SPO, and torrefaction followed by pyrolysis (SPO and FPO T225, T250, and T275) were also analyzed to determine the effect of torrefaction on intermediate bio-oil characteristics.

Table 3. Experimental Design Parameters

	factor 1		factor 2	factor 3
feedstock	pretreatment temperature (°C)	pyrolysis temperature (°C)	pyrolysis heating rate (°C/s)	catalytic upgrading temperature (°C)
PC T100	100	500	0.13, 100	400, 450, 500
PC T225	225	500	0.13, 100	400, 450, 500
PC T250	250	500	0.13, 100	400, 450, 500
PC T275	275	500	0.13, 100	400, 450, 500

Yields of individual byproduct components, coke, tar, and char (by difference), were determined. Tar was considered to be the toluene/acetone/methanol-soluble material adhered to the catalyst and was quantified by washing the catalyst with a solvent mixture containing equal parts toluene, acetone, and methanol (TAM) after catalytic runs, drying the catalyst, and measuring the change in mass. Catalyst coke formation was determined by heating the washed catalyst in a thermogravimetric analyzer (TGA) at 10 °C min^{-1} to 650 °C under oxygen flow. The change in the mass of catalyst was assumed to be due to the complete combustion of coke. The weight of reactor char was then determined as the difference between reactor weight change and combined coke and tar weight.

Yield Calculations. Yields were calculated relative to bio-oil fed or dry PC feedstock or as follows:

$$Y_i\ (\%,\ \text{w/w of bio-oil}) = \frac{\text{product}_i\ (\text{g})}{\text{bio-oil fed (g)}} \times 100 \quad (1)$$

$$Y_i\ (\%,\ \text{w/w of dry PC}) = \frac{Y_i\ (\%,\ \text{w/w of bio-oil}) Y_{\text{torrefaction}} Y_{\text{pyrolysis}}}{100^2} \quad (2)$$

where Y_i is the yield of product i (e.g., whole liquid, oily phase, aqueous phase, chemical components, coke, char, and tar), $Y_{\text{torrefaction}}$ is the yield of solid torrefied PC (%, w/w) for the particular treatment, and $Y_{\text{pyrolysis}}$ is the yield of liquid intermediate (%, w/w) from pyrolysis.

Product Characterization. Chemical composition was determined using calibrated gas chromatography−mass spectrometry (GC−MS) and high-performance liquid chromatography (HPLC) methods. The calibrated GC−MS method was used to determine the concentration of proposed reactants, including guaiacol and creosol, on 6-point calibrations with pure compound mixtures with an internal standard, heptane. The GC−MS system consisted of an Agilent gas chromatograph (model HP-6890) containing a HP-5 MS column, 30 m in length, with a 0.25 mm inner diameter and 0.25 μm film thickness, in conjunction with a Hewlett-Packard mass spectrometer (model HP-5973) with a mass selective detector. Upon calculating peak areas relative to heptane and using the calibration factors from the standard calibration curve, component concentrations in the product liquid were found for all samples from each process condition combination. A HPLC system (Shimadzu) was used to determine the concentrations (g L^{-1}) of major water-soluble compounds, including levoglucosan, acetic acid, formic acid, 5-hydroxymethylfurfural, and furfural using a calibrated method in feedstock bio-oils and oils upgraded at 450 °C. Aqueous samples for HPLC analysis were generated by mixing oily phase bio-oil with water at a 1:1 ratio, centrifuging the mixture, and then taking a sub-sample of the upper aqueous phase for analysis.

Post-run Catalyst Characterization. After each catalytic process, a sub-sample of TAM-washed catalyst was taken for surface area analysis, as described previously in the Catalyst Preparation section, to determine how processing conditions impacted surface area, pore radius, and pore volume as a result of the formation of coke. We also compared the surface chemistry of the catalysts prior to and after processing using temperature-programmed desorption (TPD) of NH_3 in the same Quantachrome Autosorb (model 1-C) analyzer used to measure surface area characteristics. The analyzer was equipped with a thermal conductivity detector (TCD) for detection of NH_3 during desorption. The intent was to show the change in acid strength and acid site density as a function of process conditions. Changes in acid site strength were assessed by comparing the temperature at which maximum desorption occurred for a low-temperature desorption event (200−300 °C) representative of weak, Lewis, acid sites and for a

higher temperature adsorption event (300−550 °C) representing strong, Brønsted, acid sites, with ranges proposed by Joo et al.[26] Changes in acid site density were assessed by comparing the peak height of the respective weak and strong acid desorption events. Prior to adsorption, samples were degassed at 300 °C for 2 h, then exposed to flowing NH_3, and heated to 500 °C at 20 °C min^{-1}. We predicted less change in the catalyst surface area, volume, pore radius, and surface chemistry parameters in catalysts from upgrading runs using torrefied feedstock for bio-oil production relative to catalysts used to process bio-oils generated from non-torrefied feedstock.

Statistical Design. The experiment was designed such that three-way analysis of variation (ANOVA) could be used to determine the effects of three factors, including pretreatment temperature (four levels at 100, 225, 250, and 275 °C, denoted T100, T225, T250, and T275, respectively), pyrolysis heating rate (two levels at 0.13 or 100 °C s^{-1}, denoted SP or FP for slow pyrolysis and fast pyrolysis, respectively), and catalytic cracking temperature (four levels at 400, 450 and 500 °C and the control, denoted as U400, U450, U500, and CTRL, respectively), on yields of byproduct, on concentration and yield of coke precursors, and on catalyst properties. The null hypothesis for all analyses was that factors at any level had no effect on the product yield, product composition, or catalyst characteristics. Rejection of the null hypothesis was concluded at p values less than a level of significance, $\alpha = 0.05$. The Holm−Sidak or Tukey method of multiple comparisons was used to compare the effects of levels for each factor.

RESULTS AND DISCUSSION

As seen in Figure 1, the pyrolysis liquid yield decreased with an increasing torrefaction temperature. The yield was maximized

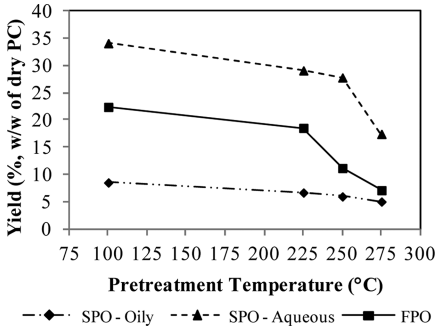

Figure 1. Yield of oily and aqueous-phase oil from pyrolysis of torrefied PC biomass relative to dry PC feedstock.

for T100 solid feedstock. This observation was as expected because torrefaction removes a portion of the volatile material that would otherwise condense with the bio-oil. The reduction in volatile content with torrefaction was observed as indicated by the characterization data in Table 1. Components of the volatile content removed were expected to be comprised of proposed coke precursors, including organic acids, aldehydes, and furans.

Effect of Processing on the Yield of Catalytic Cracking Byproducts. Torrefaction had a significant effect on the average yield (including both SP- and FP-derived products) of all byproducts of catalytic cracking noncondensable gas, aqueous-phase liquid, catalyst coke, catalyst tar, and reactor char. The gas yield significantly increased (at $\alpha = 0.05$) with an increasing pretreatment temperature for all temperature comparisons ranging from 6 to 32% for FPO and from 12.7 to 19.6% for SPO. The gas yield and liquid product yield (oily, aqueous, and whole) were not significantly correlated at $\alpha < 0.05$. The aqueous-phase yield was significantly higher (34%) for FPO relative to SPO. In addition, the aqueous-phase yield increased with an increasing torrefaction temperature, indicating that the bio-oil intermediate that was produced from torrefied biomass underwent a greater level of cracking. Yields for individual heating rates are shown in Figure 2 for tar, char, and coke. The tar yield, shown in panels A and B of Figure 2, also significantly decreased with an increasing catalytic cracking temperature for all pretreatment temperature comparisons, except for T250 (averaging 7.3%, w/w of feed) versus T275 (average at 9.0%). An increasing torrefaction temperature also significantly reduced reactor char formation (panels C and D of Figure 2) for all temperature comparisons, except for T225 versus T250. For SPO, the largest reduction in char formation was 61.2% for SP T250 U400 versus SP T100 U400. For FPO, the largest reduction was 57.8% for FP T225 U400 versus FP T100 U400.

A particularly important effect observed was a significant reduction in catalyst coke (see panels E and F of Figure 2) with an increasing pretreatment temperature for all temperature comparisons. In the best case scenario for SPO upgrading (Figure 2E), the reduction in coke (%, w/w of feed) was 28.5% relative to the respective control (SP T250 U450 versus SP T100 U450). For FPO processing (Figure 2F), the greatest reduction in coke was 34.9% (FP T275 U400 versus FP T100 U400). All torrefaction temperatures reduced coke and tar relative to T100 controls. The average coke yield (%, w/w of feed) resulting from FPO processing was 6.3%, while for SPO processing, the coke yield was 7.2%. The yield of coke for U400, U450, and U500 was 7.5, 6.3, and 6.4%, respectively. These values are similar to those observed by Vitolo et al.[10] when upgrading Swedish pine wood-derived bio-oil over HZSM-5 (Si/Al = 50) at 410−490 °C, for which the coke yield (%, w/w of bio-oil) ranged from 4.9 to 6.6%.

However, when the combined yield of coke, char, and tar was considered, some processing conditions indicated that the yield was substantially higher (see Figure 3) than the combined coke, char, and tar yield reported by Vitolo et al.,[10] which ranged from 18.3 to 29.2%. In the worst case (SPO T100 U400) observed in this study, 55.8% of bio-oil resulted in coke, char, and tar formation. Combined coke, char, and tar (CCT) was significantly reduced for SPO with an increasing torrefaction temperature for T100 versus T250 (8.8% difference; $p < 0.001$) and T100 versus T275 (7.1% difference; $p = 0.002$), reaching a minimum of 27.1% for SPO T275 U500. For FPO, CCT decreased with an increasing torrefaction temperature for T100 versus T275 (7.7% difference; $p < 0.001$), T225 versus T275 (4.7% difference; $p = 0.049$), and T250 versus T275 (9.5% difference; $p < 0.001$). For both SPO and FPO, the reduction in CCT with an increasing torrefaction temperature, particularly for T275, was proposed to be due to the increased conversion of the cellulose component of the solid feedstock, the source of levoglucosan, meaning that less levoglucosan would evolve during pyrolysis of the torrefied feedstock and less would be in bio-oil vapor passing across the catalyst bed. Levoglucosan has been indicated in the formation of unconvertible solids known as humins when processed in the presence of water and an acidic catalyst that form coke, char, and tar during processing.[30]

Catalytic cracking temperature also had a significant effect on CCT. For SPO, an increased catalytic cracking temperature reduced CCT for U400 versus U500 (16.4% difference) and U450 versus U500 (4.6% difference). Similarly, for FPO, CCT was significantly reduced with an increasing catalytic processing temperature for all temperature comparisons, indicating maxima at 37.7% (T100 U400), the least severe processing

dx.doi.org/10.1021/ef301695c | Energy Fuels 2013, 27, 844−856

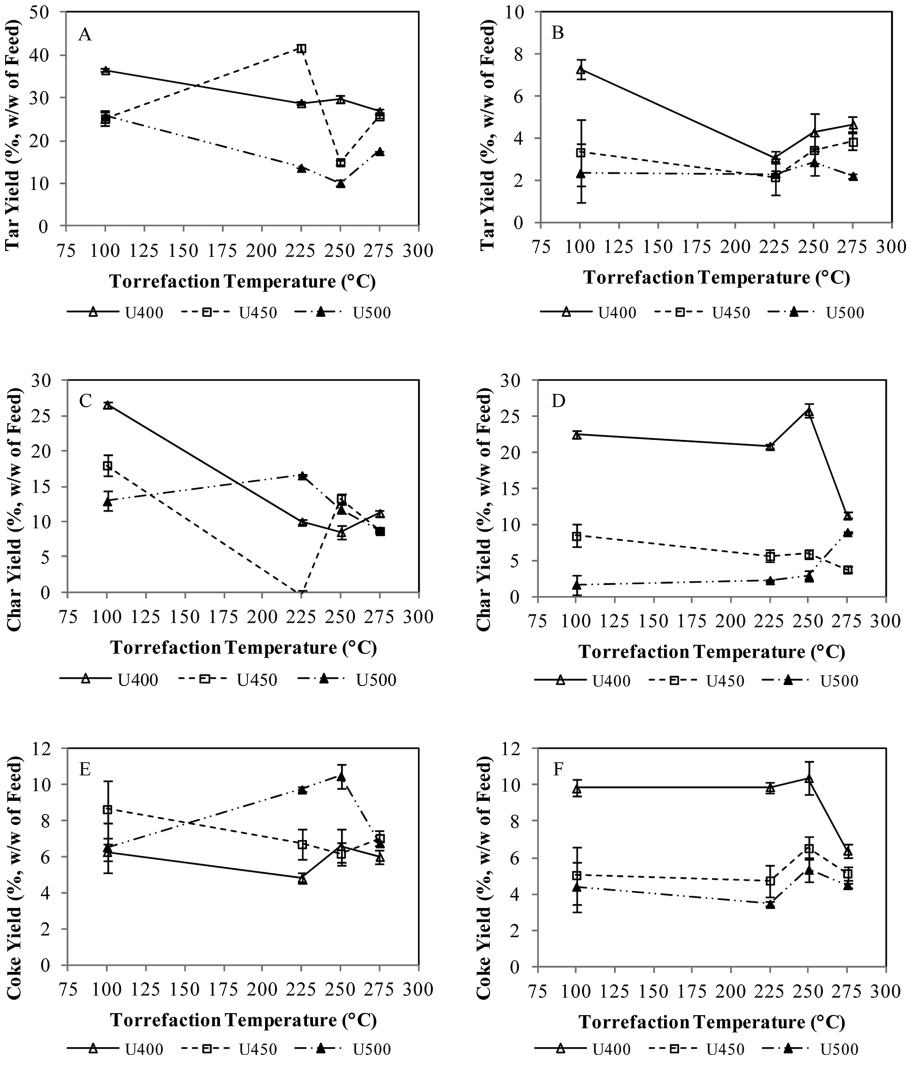

Figure 2. Yield (%, w/w of bio-oil feed) of solid products, including (A and B) tar, (C and D) reactor char, and (E and F) catalyst coke from catalytic cracking of (A, C, and E) SPO and (B, D, and F) FPO derived from PC pretreated at 100, 225, 250, and 275 °C. Error bars indicate the 95% confidence interval.

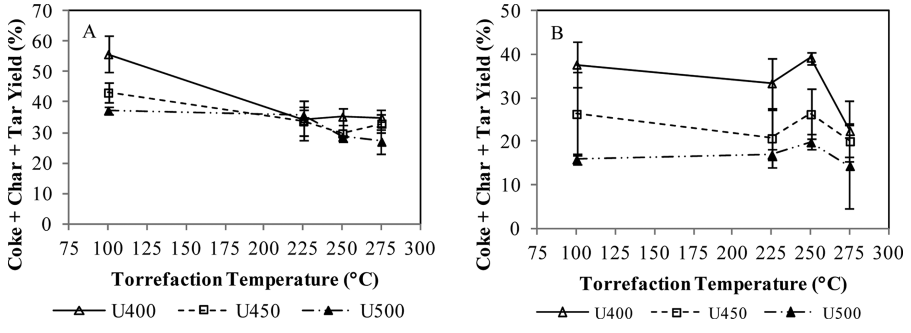

Figure 3. Combined yield (%, w/w of bio-oil feed) for (A) SPO and (B) FPO pretreated at 100, 225, 250, and 275 °C and upgraded over HZSM-5.

conditions, and 39% (T250 U400) and a minimum at 14.4% (T275 U500), the most severe conditions. For both SPO and FPO processing, the most severe reaction conditions (T275 U500) resulted in the minimization of combined coke, char, and tar relative to the quantity of bio-oil fed. However, this reduction comes at the cost of a reduced overall yield of liquid product.

Effect of Processing on Chemical Reactants. Despite lower oily phase liquid yields as a result of torrefaction, we expected to observe positive effects on intermediate bio-oil quality that would result in the reduced formation of CCT. We proposed this to be due to reduced concentrations of reactive compounds, including organic acids (formic, acetic, and lactic), aldehydes (furfural and acetaldehyde), and ketones, as indicated by Pommer et al.[21] and Prins et al.[24] Figure 4 shows the concentration of several bio-oil chemical components, including levoglucosan (Figure 4A), formic acid (Figure 4B), acetic acid (Figure 4C), 5-hydroxymethylfurfural (5-HMF; Figure 4D),

dx.doi.org/10.1021/ef301695c | Energy Fuels 2013, 27, 844−856

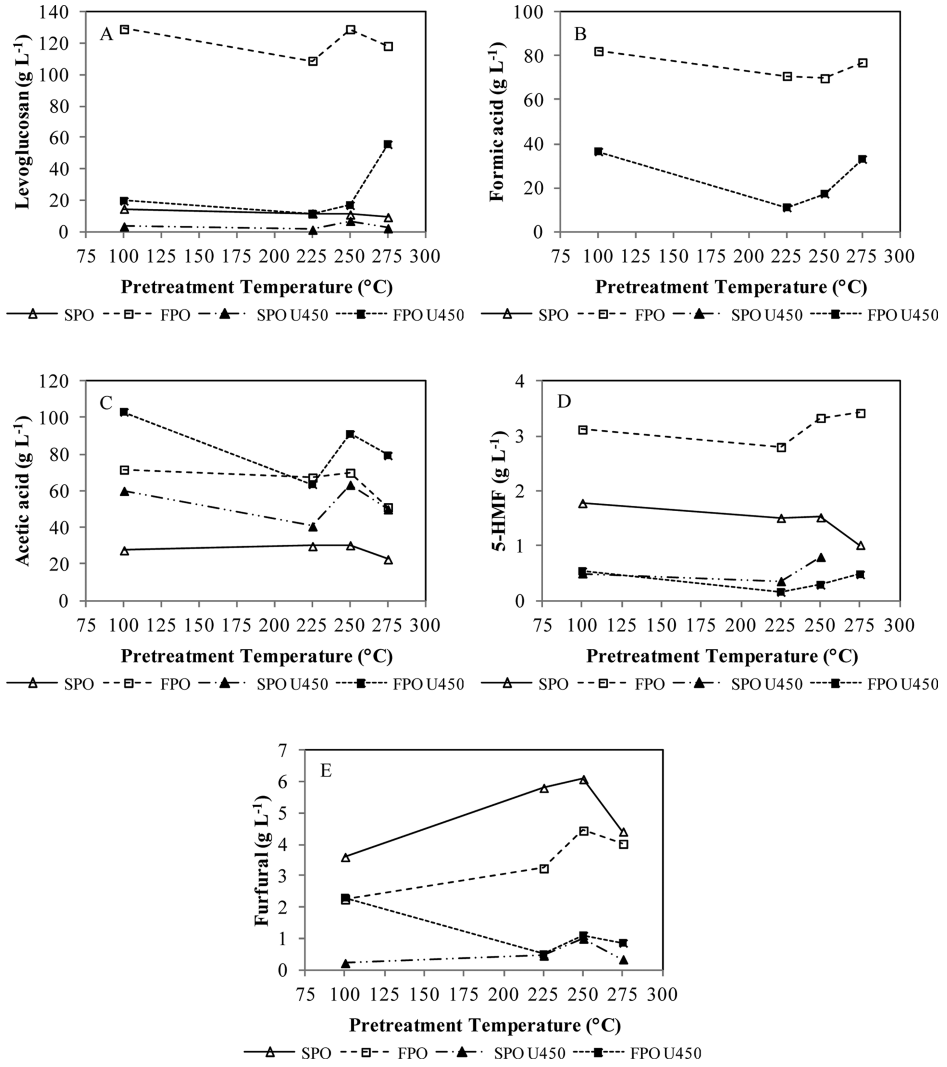

Figure 4. Concentration (g L^{-1}) of select components in bio-oil generated from feedstock pretreated at 100, 225, 250, and 275 °C prior to and after catalytic cracking over HZSM-5 as determined by HPLC.

and furfural (Figure 4E), before and after catalytic processing at U450. The pyrolysis heating rate was a highly significant predictor of the concentration of each of these components. For the SPO feed, the average concentrations of levoglucosan, formic acid, acetic acid, 5-HMF, and furfural were 11.7, 0.0, 27.6, 1.46, and 5.0 g L^{-1}, respectively, while for FPO feed, the average concentrations were 121.4, 75.0, 65.0, 3.2, and 3.5 g L^{-1}, respectively. For each reactant, except furfural, the concentration was significantly higher in FPO feed compared to the SPO feed. Additionally, the concentration of furfural increased with the torrefaction temperature (p = 0.042) from an average minimum of 2.1 g L^{-1} to a maximum of 3.2 g L^{-1}, while all other reactants were statistically unaffected by torrefaction. Of interest to note was that the concentration of levoglucosan, a product of cellulose decomposition, did not change as a function of the torrefaction temperature, but this was due to the reduced overall yield of liquid with increasing torrefaction severity. As indicated in the following section, the yield of levoglucosan did reduce with an increasing torrefaction temperature.

When the yield of chemical components was determined (shown in Figure 5), an entirely different trend was observed. For the FPO intermediate (no cracking), significant and substantial reduction in the yield was seen for levoglucosan (R^2 = 0.95; p = 0.024), formic acid (R^2 = 0.95; p = 0.025), acetic acid (R^2 = 0.90; p = 0.052), and 5-HMF (R^2 = 0.94; p = 0.029) with an increasing torrefaction temperature. Furfural (R^2 = 0.47; p = 0.315) showed no significant relationship with the torrefaction temperature. For the SPO intermediate, yields of levoglucosan (R^2 = 0.99; p = 0.006), acetic acid (R^2 = 0.85; p = 0.077), and 5-HMF (R^2 = 0.95; p = 0.025) were also highly correlated with the torrefaction temperature. Furfural, as with FPO, showed no significant correlation (R^2 = 0.30; p = 0.453) with the torrefaction temperature, and there was no formic acid detected in SPO. The concurrent reduction in the intermediate whole liquid yield partly explains why no correlation was observed between the component concentration and coke yield previously detailed. The reduction in the yield of bio-oil components supports the hypothesis that torrefaction removes coke precursors. However, as indicated in subsequent sections, these components were not well-correlated with coke formation, meaning that, although the concentration may have been reduced in the intermediate feedstock, the coke yield did not necessarily follow the same trend.

The concentrations for two additional reactants, phenolic monomers, guaiacol and creosol, are provided in panels A–D

dx.doi.org/10.1021/ef301695c | Energy Fuels 2013, 27, 844–856

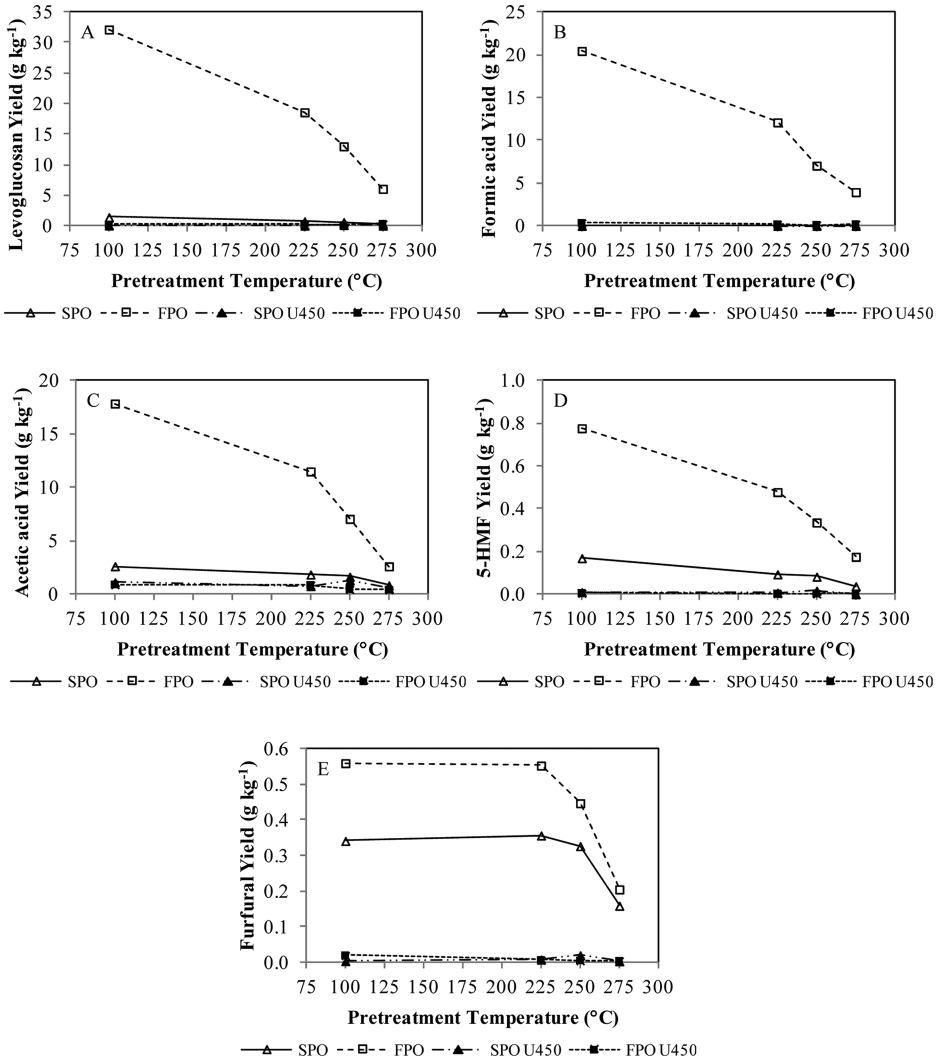

Figure 5. Yield (g kg^{-1} of dry PC) of select components in bio-oil generated from feedstock pretreated at 100, 225, 250, and 275 °C prior to and after catalytic cracking over HZSM-5 as determined by HPLC.

of Figure 6 for oil feedstocks and catalytically cracked products. For bio-oil feedstock (non-cracked), the guaiacol concentration was shown to be significantly (R^2 = 0.757; p = 0.005) related to the heating rate but not the torrefaction temperature. The concentration for guaiacol was lower in FPO (29.4 g L^{-1}) compared to SPO (39.0 g L^{-1}). For creosol, the concentration was significantly lower (R^2 = 0.74; p = 0.006) in FPO (41.2 g L^{-1}) compared to SPO (46.5 g L^{-1}).

Effect of the Reactant Concentration on the Coke Yield. To determine which of the reactants measured in SPO and FPO prior to upgrading were significant predictors of the coke yield upon catalytic processing at U450, backward stepwise regression was used with independent variables, including levoglucosan, furfural, 5-HMF, acetic acid, formic acid, guaiacol, and creosol concentrations. Analysis indicated that, of the independent variables, the concentrations of levoglucosan, 5-HMF, acetic acid, formic acid, guaiacol, and creosol were not significant predictors of catalyst coke for U450 bio-oils at α = 0.05. However, of the remaining dependent variables, the concentrations of formic acid and furfural were highly significant (R^2 = 0.84; p = 0.01) predictors of catalyst coke. However, the coke yield was reduced with an increasing concentration of formic acid and furfural. This result was not as expected, particularly with furfural. This observation did not indicate that 5-HMF, acetic acid, formic acid, guaiacol, and creosol concentrations were not coke promoters or precursors or that minimizing the concentration of these components in bio-oil feedstock reduced coke formation. However, the increase in formic acid and furfural concentrations and corresponding reduction in coke with an increasing torrefaction temperature indicated that torrefaction pretreatment reduced coke not by reducing the concentration of a proposed coke precursor but by increasing concentration of the components, formic acid and furfural, in this case. For formic acid, the reduction in coke with an increasing concentration could be explained by the fact that formic acid thermally decomposes to H_2, acting as an *in situ* hydrogen donor, an effect that has been shown in previous studies.[31] The presence of H_2 from a hydrogen donor, such as formic acid, would result in reduced coking because of reactions between H_2 and bio-oil cracking intermediates prior to the formation of coke.[32,33] Torrefaction did not significantly reduce the concentration on any of the other reactants in the intermediate bio-oil, including levoglucosan, formic acid, acetic acid, 5-HMF, guaiacol, or creosol.

dx.doi.org/10.1021/ef301695c | *Energy Fuels* 2013, 27, 844−856

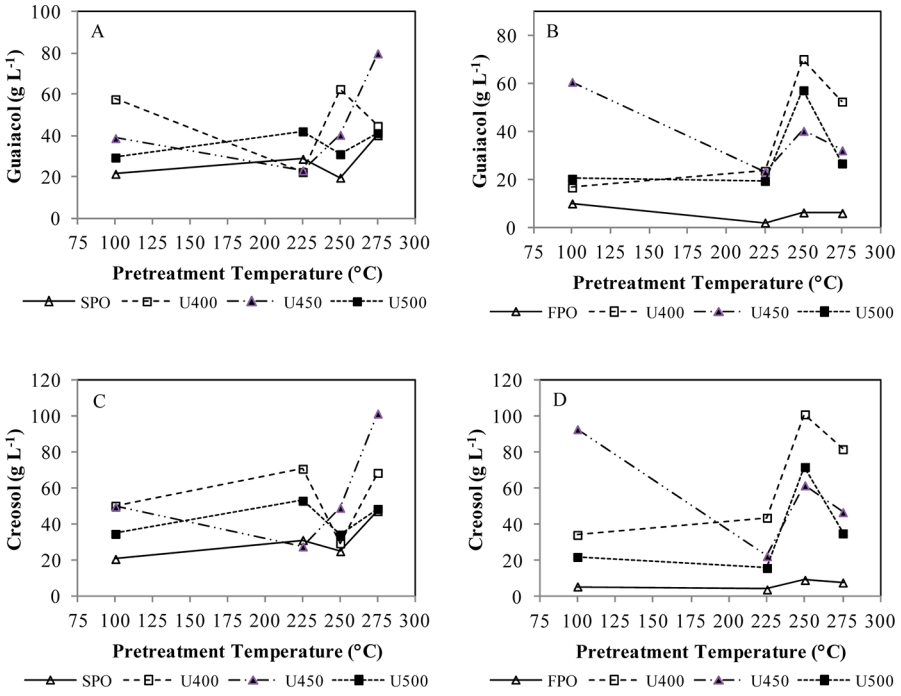

Figure 6. Concentration (g L^{-1}) of (A and B) guaiacol and (C and D) creosol in (A and C) SPO and (B and D) FPO generated from feedstock pretreated at 100, 225, 250, and 275 °C prior to and after catalytic cracking over HZSM-5 as determined by GC−MS.

In contrast, the CCT yield (%, w/w of feed), shown in Figure 3, from U450 processing was significantly affected (R^2 = 0.993; p = 0.017) by the torrefaction temperature and reactant concentrations, including those of levoglucosan, formic acid, acetic acid, and furfural. CCT decreased with an increasing torrefaction temperature, with decreasing formic acid, acetic acid, and furfural concentrations, and with an increasing levoglucosan concentration in feed bio-oil. Although not measured here, we believe this decrease in CCT with an increasing levoglucosan concentration was due to the fact that, as the torrefaction temperature increased, concentrations of cellulose-derived oligomers and polymers, including cellobiose, compounds that generate solid byproducts, were reduced in concentration because of greater conversion to levoglucosan. Thus, feedstock oils from more severely torrefied biomass indicated higher concentrations of levoglucosan, while those from less severely treated feedstock would, in theory, have higher concentrations of CCT-generating oligomers. The CCT yield was smallest for FPO pretreated at T275 at 20.1% (w/w of bio-oil feed). Torrefaction as a pretreatment clearly and positively impacted the formation of catalytic cracking byproducts for both slow- and fast-pyrolysis bio-oil.

Effect of Process Conditions on Catalyst Surface Characteristics. Figure 7 shows the variation in catalyst characteristics, including surface area (m^2 g^{-1}, panels A and B of Figure 7), average pore radius (Å, panels C and D of Figure 7), and pore volume (cm^3 g^{-1}, panels E and F of Figure 7). For fresh catalyst, these values were 343, 10.81, and 0.185, respectively. It is clear from the graphs that both surface area and pore volume significantly decreased as a result of catalytic processing. The average pore radius actually increased for all processing conditions. The highest average pore radius observed was 12.03 Å for FPO processing of PC T275 U400. An increase in pore radius indicates that small pores have been blocked by coke. Small pore blockage resulted in a concurrent reduction in surface area and pore volume.

Upon further inspection of the effect of catalytic processing on pore size (Figure 8), it was clear from the BJH plots [D_v(log r) versus radius] that not only small pores but also larger pores had been filled and blocked. For SPO processing (panels A, C, and E of Figure 8), both small pores (∼10 Å) and larger pores (∼18 Å) experienced a decrease in concentration with increasing catalytic processing. For FPO, the opposite was true; i.e., small and large pore site density increased with an increasing catalytic processing temperature.

Each of these phenomena, i.e., reductions in surface area and pore volume and increases in average pore radius, indicate that detrimental, although not necessarily irreversible, changes have occurred to the catalysts. As such, conditions that minimize these changes are considered optimal. A simple comparison technique (see eq 3) was devised to determine the catalyst effectiveness for minimizing changes to average pore radius, pore volume, and surface area. The equation used was

$$C_{\text{eff,surface}} = \left[\frac{1}{\text{pore size}} + \text{pore volume} + \ln(\text{surface area})\right]_i \Big/ \left[\frac{1}{\text{pore size}} + \text{pore volume} + \ln(\text{surface area})\right]_{\text{fresh}} \quad (3)$$

Table 4 shows the results from this comparison. The highest effectiveness for minimizing catalyst changes calculated (0.89) was for SPO processed under the least severe conditions, i.e., T100 U400. For SPO under all other torrefaction temperature processing, catalytic cracking at 400 °C maximized effectiveness. For FPO processing, the opposite was true; i.e., the highest effectiveness (at 0.78) was seen for the most severe pretreatment and catalytic cracking conditions, T275 U500. The opposing phenomena for SPO and FPO correlate well with the accumulation of catalyst coke, wherein the coke yield

dx.doi.org/10.1021/ef301695c | Energy Fuels 2013, 27, 844−856

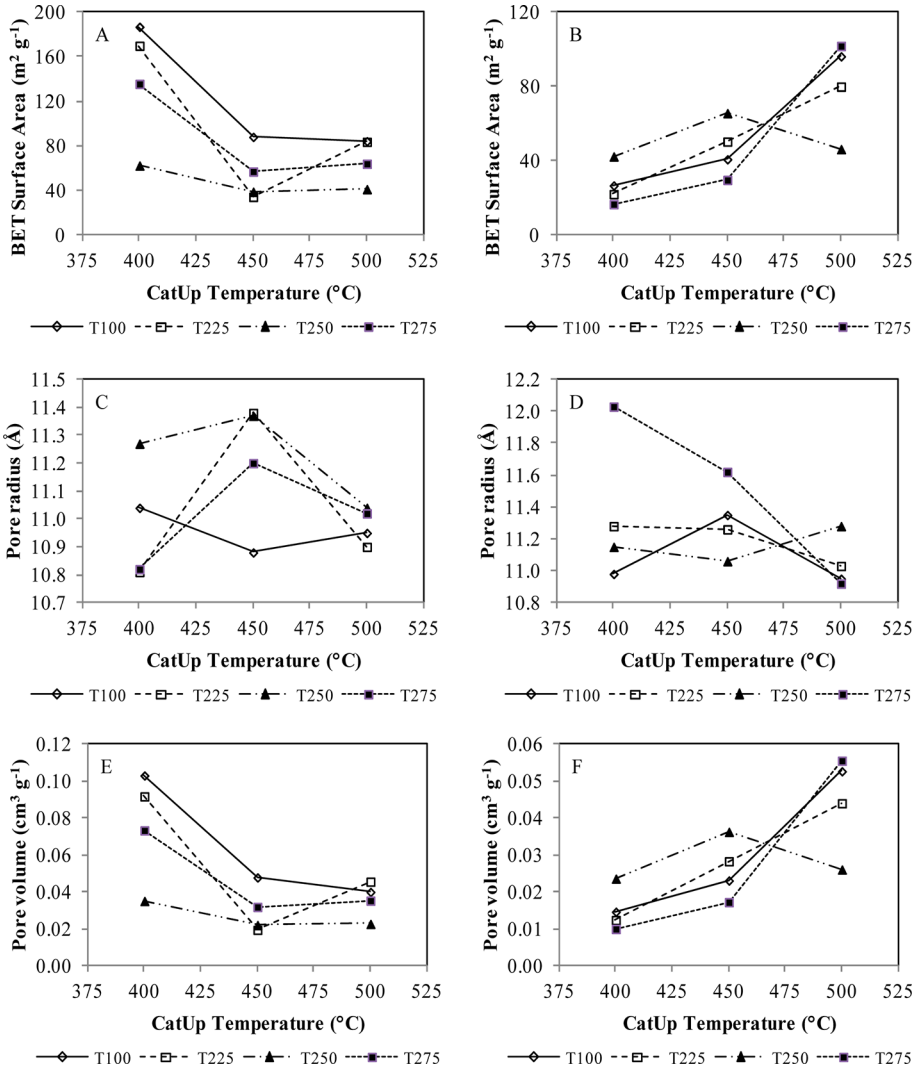

Figure 7. Variation in the catalyst surface area, average pore radius, and pore volume upon HZSM-5 processing of (A, C, and E) SPO and (B, D, and F) FPO derived from PC pretreated at 100, 225, 250, and 275 °C.

increased or remained flat for SPO and decreased for FPO with increasing catalytic cracking severity.

We suspected that the differing effect of SPO versus FPO processing on catalyst properties was due to the nature of the HZSM-5 catalyst, the concentration of levoglucosan in the bio-oil feedstock, and the degree of lignin depolymerization in the feedstock. The medium pore size HZSM-5 catalyst used readily supports adsorption and desorption of monoaromatics, while restricting polyaromatics.[4] For SPO, the low heating rate and long residence time during pyrolysis and secondary cracking correspond to more severe degradation of parent lignin to phenolic monomers (monoaromatics). These monomers (light organics) are less restricted in the small pores of the catalyst and are thus less likely to collect and form coke. To confirm the theory that SPO had a higher level of phenolic monomers, yields of guaiacol (2-methoxyphenol) and creosol (2-methoxy-4-methylphenol) were compared between SPO and FPO. These results are shown in Figure 9. Although there was no significant difference in the yield for guaiacol, the difference for creosol was significant, with SPO being substantially higher. In addition, for FPO, the yield of both phenolic monomers decreased with an increasing pretreatment temperature, indicating enhanced conversion to products and byproducts as a result of pretreatment. Without quantification of additional phenols, however, it would be difficult to conclude if monomeric phenolic content was higher overall in SPO or FPO.

Following the reaction pathway proposed by Adjaye and Bakhshi[4] for acidic zeolite catalyst, light organics are deoxygenated, cracked, oligomerized, aromatized, alkylated, and isomerized to form aromatic hydrocarbons under the less severe cracking conditions used here, i.e., 400 °C versus 500 °C. At higher severity cracking, aromatic hydrocarbons polymerize to form coke and tar. For FPO, a larger fraction of lignin remains in oligomer form (heavy organics). At lower catalytic processing temperatures, the oligomers collect in and around the catalyst pores and polymerize, blocking the channels and pores and allowing for the buildup of more coke. The reduction in coke with an increasing temperature was evident in Figure 2 for FPO processing. For SPO, the longer residence time (i.e., higher severity) during pyrolysis generated an intermediate product that more readily reacted (i.e., higher reaction rate) to form aromatics during cracking. The increased reaction rate for SPO versus FPO means that aromatics had a longer residence time in the catalyst bed, during which time polymerization occurred, forming greater amounts of coke. At

dx.doi.org/10.1021/ef301695c | Energy Fuels 2013, 27, 844−856

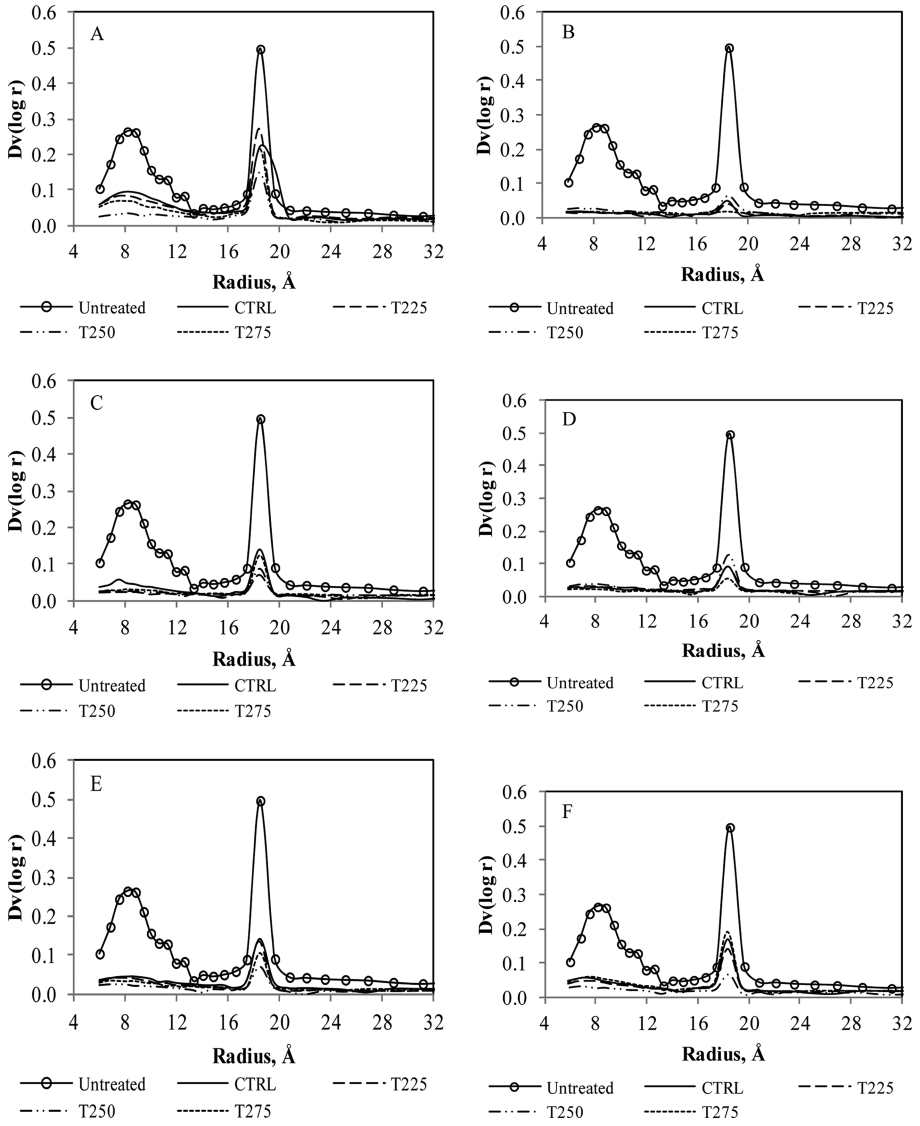

Figure 8. BJH plots showing pore size distribution for HZSM-5 after catalytic processing at (A and B) 400 °C, (C and D) 450 °C, and (E and F) 500 °C for (A, C, and E) SPO and (B, D, and F) FPO.

Table 4. Catalyst Effectiveness (0−1) for Minimizing Changes in Surface Area, Pore Radius, and Pore Volume

process temperature (°C)		relative effectiveness	
torrefaction	catalytic upgrading	SPO	FPO
	400	0.89	0.55
100	450	0.76	0.62
	500	0.75	0.77
	400	0.87	0.52
225	450	0.60	0.66
	500	0.75	0.74
	400	0.70	0.63
250	450	0.62	0.70
	500	0.63	0.65
	400	0.83	0.48
275	450	0.68	0.57
	500	0.70	0.78

higher temperatures, the oligomers begin to decompose (crack) first to light organics (mono- and biaromatic phenols), which then more readily pass through the catalyst channels and adsorb/desorb in pores, eventually forming aromatic hydrocarbons.

Effect of Process Conditions on Catalyst Surface Activity. Figure 10 shows the variation in the relative amount of desorbed NH_3 during TPD analysis of fresh ("untreated") and used HZSM-5 catalyst after processing SPO (Figure 10A) and FPO (Figure 10B) at 450 °C. After processing, U450 catalysts, regardless of feedstock preprocessing conditions, showed reduced adsorption capacity for both weak acid (adsorption peak between 250 and 260 °C) and strong acid (adsorption peak between 420 and 440 °C) sites relative to unused catalyst in temperature ranges proposed by Joo et al.[26] from HZSM-5. Among pretreatment temperatures, differences were also evident. NH_3 adsorption capacity appeared to be slightly higher for both weak and strong acid sites for catalysts used for processing SPO relative to FPO. However, a multiple comparison of ranks for the treatments using Tukey's method indicated that NH_3 absorption for the weak acid site was not statistically different for SP versus FP. Conversely, the average adsorption signal for the weak sites on SPO T225, T250, and T275 catalysts at 11.8, 12.5, and 14.1 mV, respectively, showed

dx.doi.org/10.1021/ef301695c | Energy Fuels 2013, 27, 844−856

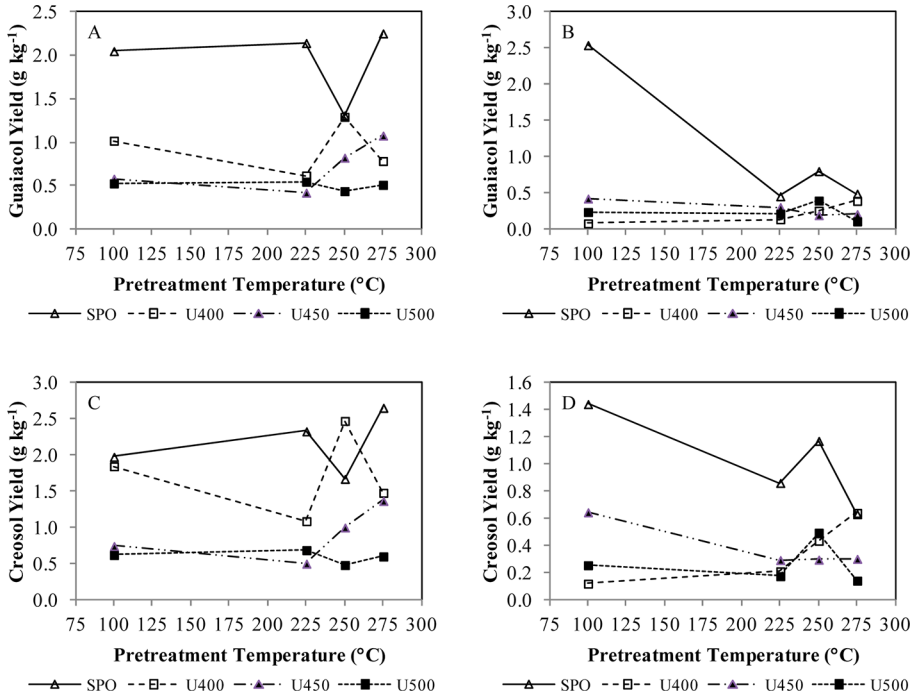

Figure 9. Yield (g kg^{-1} of dry PC) of (A and B) guaiacol and (C and D) creosol in (A and C) SPO and (B and D) FPO derived from PC pretreated at 100, 225, 250, and 275 °C prior to pyrolysis and catalytic processing.

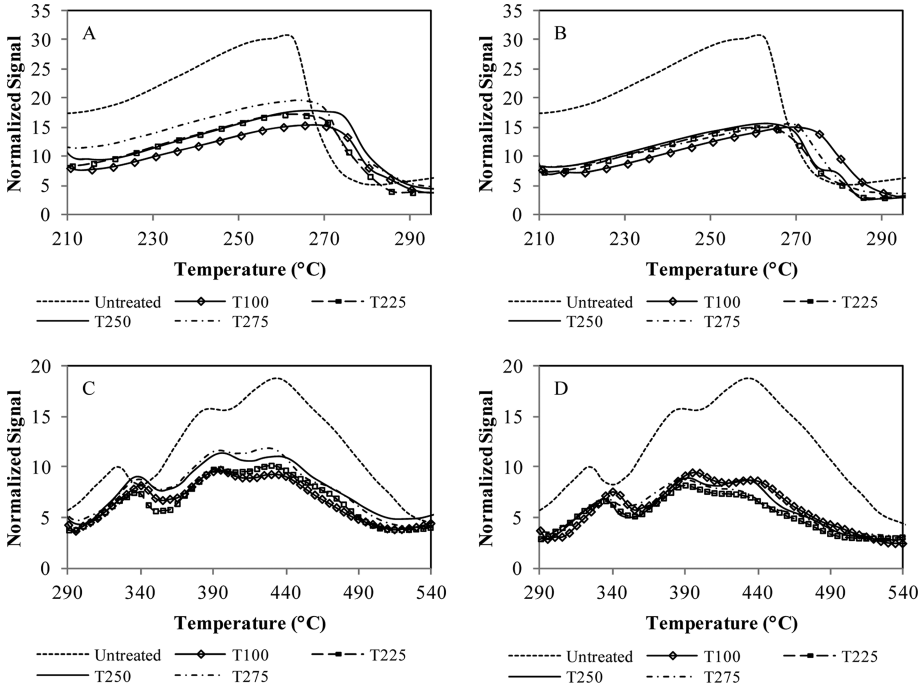

Figure 10. NH_3-TPD results for HZSM-5 catalyst used to process (A and C) SPO and (B and D) FPO derived from pyrolysis of feedstock pretreated at 100, 225, 250, and 275 °C at a catalytic cracking temperature of 450 °C.

no significant difference from the untreated catalyst at 19.4 mV. SPO T100 was significantly different at 10.9 mV. Weak acid site density increased with an increasing torrefaction temperature for SPO. For FPO, ammonia adsorption for the weak sites was lower than for the fresh catalyst for catalysts from T100, T225, T250, and T275 at 9.8, 10.4, 10.4, and 10.3 mV, respectively, indicating greater deactivation of weak acid sites compared to respective SPO catalysts. For FPO catalytic processing, torrefaction pretreatment resulted in used catalyst with greater weak acid site density than for non-torrefied biomass, although among torrefaction temperatures, no difference was seen.

For the strong acid site (290−490 °C; panels C and D of Figure 10), greater differences were indicated. All pretreated catalysts, from both SPO and FPO, were significantly different from the fresh catalyst at 12.2 mV. For SPO, the median values for T100, T225, T250, and T275 were 7.0, 7.1, 8.2, and 8.2, respectively, indicating in increase in strong acid site density particularly for T250 and T275. For FPO, values were 6.4, 5.7,

dx.doi.org/10.1021/ef301695c | *Energy Fuels* 2013, 27, 844−856

5.8, and 6.1 mV. Adsorption capacity for SPO T250 (median at 9.34 mV) and SPO T275 (9.02 mV) was significantly higher ($p < 0.05$) than for all FPO treatments, indicating less reduction in catalytic activity for catalysts from T250 and T275 after processing SPO. At T225, SPO catalysts also indicated significantly higher adsorption capacity then for FPO T225 but not for any other FPO pretreatment temperature. Within the SPO and FPO groups, no difference in activity was indicated between T225, T250, and T275 and the control, T100, despite the increased level of coke in the T100 catalyst.

The reduction in NH_3 adsorption for used catalyst was assumed to be mainly the result of catalyst coke blocking acidic pore sites. This conclusion was based on the fact that the temperature of maximum desorption for peaks representing both weak and strong sites changed very little as a result of bio-oil processing. Only the signal intensity changed, indicating a change in acid site density and not a change in pore chemistry. In addition, regeneration of the catalyst by heating under oxygen (data not shown) completely renewed the catalyst, such that no difference NH_3 adsorption was evident between the unused and used catalyst.

CONCLUSION

It was clear that torrefaction pretreatment affected in a variety of ways the formation of byproducts and the properties and function of the HZSM-5 catalyst upon upgrading fast- and slow-pyrolysis bio-oil derived thereof. It was previously shown[29] that torrefaction pretreatment significantly reduced average yields (%, w/w of feed) of catalytic cracking byproducts, including reactor char, catalyst coke, and catalyst tar, relative to the best-case conditions using non-torrefied feedstock. It was proposed here that the reductions in the byproduct yield were the effect of reduced concentrations of coke precursors in intermediate bio-oils, including organic acids (acetic and formic), aldehydes (5-HMF and furfural), and oxyphenols (guaiacol and creosol). However, in terms of concentration, only furfural showed a significant correlation with the torrefaction temperature and only furfural and formic acid indicated correlations, inverse in this case, with coke formation.

Although torrefaction and supposed coke precursor concentrations for the most part had no significant effect on coke singularly, torrefaction significantly impacted the combined coke, char, and tar yield by decreasing the yield with an increasing torrefaction temperature, with decreasing formic acid, acetic acid, and furfural concentrations, and with an increasing levoglucosan concentration, reaching a minimum of 14.4% (w/w of bio-oil feed) for FPO T275 U500 compared to 39.2% for the worst-case scenario. The combined coke, char, and tar may actually represent a better metric to assess the effects of torrefaction pretreatment because all of these byproducts can conceivably hinder the effectiveness of catalytic cracking with respect to end-product quality, catalyst longevity, and process viability and scalability.

Torrefaction also improved catalyst effectiveness for minimizing changes to pore size, pore volume, and surface area upon upgrading FPO but reduced effectiveness for SPO processing. Torrefaction of biomass prior to slow pyrolysis significantly improved weak and strong acid site density after catalytic processing, although no clear effect was seen for FPO-processing catalysts. With respect to catalyst function, acidity in particular, torrefaction pretreatment had a predominantly positive effect on the weak and strong acid site density of HZSM-5 after processing of both SPO and FPO.

All in all, torrefaction had a positive impact on the yield of coke, char, and tar and catalyst activity. Although longevity was not measured here, increased catalyst activity after processing, particularly for higher torrefaction temperatures, indicates that torrefaction should improve longevity. In subsequent work, we will determine if this is the case. It is as-yet unclear whether the reduction in byproducts and improvement in catalyst functionality overshadow the reduction in overall liquid yield with torrefaction. Additional work is needed to clarify the possibility of improvement. However, one way to improve overall yields of products would be to gainfully use the condensable liquid product from the torrefaction process, which contains various forms of pinene, a potential fuel feedstock. We are currently pursuing this avenue to improve the overall efficiency of the torrefaction pretreatment pathway.

AUTHOR INFORMATION

Corresponding Author

*Telephone: +1-706-542-0940. Fax: +1-706-542-8806. E-mail: rog@uga.edu.

Notes

The authors declare no competing financial interest.

ACKNOWLEDGMENTS

The authors graciously thank Joby Miller and Andrew Smola for their invaluable contributions of time and effort in analyzing materials. This work was supported by a U.S. Department of Energy Biorefinery Research Project grant.

REFERENCES

(1) Chen, G.; Andries, J.; Luo, Z.; Spliethoff, H. Biomass pyrolysis/gasification for product gas production: The overall investigation of parametric effects. *Energy Convers. Manage.* **2003**, *44*, 1875−1884.

(2) Carlson, T.; Cheng, Y.; Jae, J.; Huber, G. Production of green aromatics and olefins by catalytic fast pyrolysis of wood sawdust. *Energy Environ. Sci.* **2011**, *4*, 145−161.

(3) Valle, B.; Gayubo, A.; Atutxa, A.; Alonso, A.; Bilbao, J. Integration of thermal and catalytic transformation for upgrading biomass pyrolysis oil. *Int. J. Chem. React. Eng.* **2007**, *5*, 1−10.

(4) Adjaye, J.; Bakhshi, N. Production of hydrocarbons by catalytic upgrading of a fast pyrolysis bio-oil. Part II: Comparative catalyst performance and reaction pathways. *Fuel Process. Technol.* **1995**, *45*, 185−202.

(5) Adjaye, J.; Bakhshi, N. Production of hydrocarbons by catalytic upgrading of a fast pyrolysis bio-oil. Part I: Conversion over various catalysts. *Fuel Process. Technol.* **1995**, *45*, 161−183.

(6) Lu, Q.; Zhang, Y.; Tang, Z.; Li, W.; Zhu, X. Catalytic upgrading of biomass fast pyrolysis vapors with titania and zirconia/titania based catalysts. *Fuel* **2010**, *89*, 2096−2103.

(7) Corma, A.; Huber, G.; Sauvanaud, L.; O'Connor, P. Processing biomass-derived oxygenates in the oil refinery: Catalytic cracking (FCC) reaction pathways and role of catalyst. *J. Catal.* **2007**, *247*, 302−327.

(8) Park, H.; Heo, H.; Jeon, J.; Kim, J.; Ryoo, R.; Jeong, K.; Park, Y. Highly valuable chemicals production from catalytic upgrading of radiate pine saw dust-derived pyrolytic vapors over mesoporous MFI zeolites. *Appl. Catal., B* **2010**, *95*, 365−373.

(9) Elliott, D. C.; Neuenschwander, G. G. Liquid fuels by low-severity hydrotreating of biocrude. In *Developments in Thermochemical Biomass Conversion*; Bridgwater, A. V., Boocock, D. G. B., Eds.; Blackie Academic and Professional: London, U.K., 1997; Vol. *1*, pp 611−621.

(10) Vitolo, S.; Bresci, B.; Seggiani, M.; Gallo, M. Catalytic upgrading of pyrolytic oils over HZSM-5 zeolite: Behaviour of the catalyst when used in repeated upgrading−regenerating cycles. *Fuel* **2001**, *80*, 17−26.

(11) Rao, M.; Soni, D.; Sieli, G. Convert bottom-of-the-barrel into diesel and light olefins. *Hydrocarbon Process.* **2011**, 45−49.
(12) Gayubo, A.; Aguayo, A.; Atutxa, A.; Valle, B.; Bilbao, J. Undesired components in the transformation of biomass pyrolysis oil into hydrocarbons on an HZSM-5 zeolite catalyst. *J. Chem. Technol. Biotechnol.* **2005**, *80*, 1244−1251.
(13) Gagnon, J.; Kaliaguine, S. Catalytic hydrotreatment of vacuum pyrolysis oils from wood. *Ind. Eng. Chem. Res.* **1988**, *27* (10), 1783−1788.
(14) Laurent, E.; Delmon, B. Study of the hydrodeoxygenation of carbonyl, carboxylic and guaiacyl groups over sulfided CoMo/γ-Al_2O_3 and NiMo/γ-Al_2O_3 catalysts: I. Catalytic reaction schemes. *Appl. Catal., A* **1994**, *109* (1), 77−96.
(15) Centeno, A.; Laurent, E.; Delmon, B. Influence of the support of CoMo sulfide catalysts and of the addition of potassium and platinum on the catalytic performances for the hydrodeoxygenation of carbonyl, carboxyl, and guaiacol-type molecules. *J. Catal.* **1995**, *154*, 288−298.
(16) Wildschut, J.; Mahfud, F.; Venderbosch, R.; Heeres, H. Hydrotreatment of fast pyrolysis oil using heterogeneous noble-metal catalysts. *Ind. Eng. Chem. Res.* **2009**, *48*, 10324−10334.
(17) de Wild, P.; Uil, H.; Reith, J.; Kiel, J.; Heeres, H. Biomass valorisation by staged degasification: A new pyrolysis-based thermochemical conversion option to produce value-added chemicals from lignocellulosic biomass. *J. Anal. Appl. Pyrolysis* **2009**, *85*, 124−133.
(18) Zheng, A.; Zhao, Z.; Chang, S.; Huang, Z.; He, F.; Li, H. Effect of torrefaction temperature on product distribution from two-staged pyrolysis of biomass. *Energy Fuels* **2012**, *26* (5), 2968−2974.
(19) Meng, J.; Park, J.; Tilotta, D.; Park, S. The effect of torrefaction on the chemistry of fast-pyrolysis bio-oil. *Bioresour. Technol.* **2012**, *111*, 439−446.
(20) Bergman, P.; Keil, J. Torrefaction for biomass upgrading. *Proceedings of the 14th European Biomass Conference and Exhibition*; Paris, France, Oct 17−21, 2005.
(21) Pommer, L.; Gerber, L.; Olofsson, I.; Wiklund-Lindstrom, S.; Nordin, A. Gas composition from biomass torrefaction—Preliminary results. *Proceedings of the 19th European Biomass Conference and Exhibition*; Berlin, Germany, June 6−10, 2011.
(22) Phanphanich, M.; Mani, S. Impact of torrefaction on the grindability and fuel characteristics of forest biomass. *Bioresour. Technol.* **2010**, *102*, 1246−1253.
(23) Mani, S.; Das, K. C.; Kastner, J. *Development of Biomass Torrefaction Technology To Produce Biocoal for Electricity Production*, Final Report to State of Georgia; Georgia Traditional Industries Program: Atlanta, GA, 2009.
(24) Prins, M.; Ptasinski, K.; Janssen, F. Torrefaction of wood: Part 2—Analysis of products. *J. Anal. Appl. Pyrolysis* **2006**, *77* (1), 35−40.
(25) Perego, C.; Bosetti, A. Biomass to fuels: The role of zeolite and mesoporous materials. *Microporous Mesoporous Mater.* **2011**, *144*, 28−39.
(26) Joo, O.; Jung, K.; Han, S. Modification of H-ZSM-5 and γ-alumina with formaldehyde and its application to the synthesis of dimethyl ether from syn-gas. *Bull. Korean Chem. Soc.* **2002**, *23* (8), 1103−1105.
(27) Gayubo, A.; Aguayo, A.; Atutxa, A.; Prieto, R.; Bilbao, J. Deactivation of a HZSM-5 zeolite catalyst in the transformation of the aqueous fraction of biomass pyrolysis oil into hydrocarbons. *Energy Fuels* **2004**, *18*, 1640−1647.
(28) National Science Foundation (NSF). *Breaking the Chemical and Engineering Barriers to Lignocellulosic Biofuels: Next Generation Hydrocarbon Biorefineries*; Huber G. W., Ed.; NSF: Washington, D.C., 2008.
(29) Hilten, R.; Speir, R.; Kastner, J.; Mani, S.; Das, K. C. Effect of torrefaction on bio-oil upgrading over HZSM-5. Part 1: Product yield, product quality, and catalyst effectiveness. *Energy Fuels* **2013**.
(30) Hu, X.; Li, C. Levulinic esters from the acid-catalysed reactions of sugars and alcohols as part of a bio-refinery. *Green Chem.* **2011**, *13*, 1676−1679.
(31) Karimi, E.; Gomez, A.; Kycia, S.; Schlaf, M. Thermal decomposition of acetic and formic acid catalyzed by red mud—Implications for the potential use of red mud as a pyrolysis bio-oil upgrading catalyst. *Energy Fuels* **2010**, *24*, 2747−2757.
(32) Trimm, D. Catalyst design for reduced coking (review). *Appl. Catal.* **1983**, *5*, 263−290.
(33) Prasomsri, T.; To, A.; Crossley, S.; Alvarez, W.; Resasco, D. Catalytic conversion of anisole over HY and HZSM-5 zeolites in the presence of different hydrocarbon mixtures. *Appl. Catal., B* **2011**, *106*, 204−211.